

Stability of Rate and Power Control Algorithms in Wireless Cellular Networks

Anders Möller and Ulf T. Jönsson, Royal Institute of Technology
Mats Blomgren and Fredrik Gunnarsson, Ericsson Research

Abstract—In radio resource management for cellular networks a trade-off has to be made between the congestion level, related to cell coverage and intercell interference, and the Quality of Service (QoS) or data rates of the users. This is implemented by using a fast inner power control loop and an outer rate control algorithm, working on a slower time scale.

Due to the distributed nature of the network, both information and control is distributed. Measurements of congestion and QoS are used in the control loops and this introduces a nonlinear feedback. Another complicating factor is that filtering, computations and information exchange in the network introduce time delays.

In this paper we propose a general high order model as a cascade system with an outer and inner control loop. The control algorithms use distributed information available in the network. The full system model includes the nonlinear feedback from congestion and QoS measurements, time delays and time scale modelling. We provide sufficient conditions for stability and convergence of the system. Our primary analysis tool is input output theory.

I. INTRODUCTION

In wireless cellular networks there are several control loops for maintaining the Quality of Service (QoS) of the users and controlling congestion in the network. We consider uplink in a CDMA cellular network, where the users transmit on the same channel. This causes an important feedback interconnection between the users for the control loops regulating on congestion and QoS.

A fast distributed inner power control loop is used to ensure that the QoS is maintained under rapidly changing radio and interference conditions. The inner power control loop tracks a reference value on the QoS by updating the transmission powers of the users. The reference QoS signal is set by a slower outer rate control loop, which makes sure that the cell coverage is maintained by tracking a congestion reference. The outer loop works on a slower time scale, but the joint dynamics cannot be neglected.

An important motivation for using an outer control loop is to prevent power rushes, where the transmission powers of the users heavily increase. It is well known that if the QoS reference value is set too high, there exist no positive transmission powers, such that the target QoS is achieved. The users will then compete with increasing transmission powers. In e.g. [11], [9] and [10] it was also shown that power rushes can be caused in the inner loop by too

aggressive control algorithms in combination with delay. In e.g. [7] it was shown that by using a Smith predictor it is possible to compensate for delay. Typically there are delays both in the inner and outer control loop, which motivates the use of higher order control laws.

While the fast power control loop has been extensively studied over the last two decades, the outer loop has drawn less attention. Previous works concern mostly the aspect of rate allocation and have often used an optimization approach, see e.g. [3] and [8]. In [8] convergence of distributed algorithms was studied, but only when assuming that the control loops work on different time scales. Joint dynamics for a type of outer loop algorithms were studied in [1] and [13]. Both considered a simplified linear system model, treating the nonlinear effects of interference and congestion feedback as additive disturbances.

The main focus of this paper is the modelling and analysis of the joint dynamics. In Section II, the congestion measure total load is defined. It will be the key concept for the outer loop control, with a similar function as Signal to Interference Ratio (SIR) in the inner control loop. The total load can be derived directly from distributed measurements of the Rise over Thermal (RoT). In a cellular network there are constraints on the RoT related to coverage issues of the cell and intercell interference. These constraints transfer directly to the total load, and motivates controlling on it.

In Section III we derive the system model in a control theoretic framework. Then, in Section IV we consider conditions for feasibility of the joint system. In Section V we perform a general stability analysis using input output tools. Sufficient conditions are given for stability and convergence of the system. Then we focus on local analysis in Section VI, where the problem structure exploited. In particular we use scaling multipliers to sharpen the results from the previous section, which also reveal a similar structure of the inner and outer loop feedback nonlinearities.

In Section VII we illustrate the gains of using an outer loop by simulations and using the derived results. In particular we show that power rushes can be prevented and we model a realistic scenario of a WCDMA network with delays and time scale difference. The paper is concluded in Section VIII. Most proofs are omitted due to space restriction, but can be found in [12].

II. SYSTEM MODEL AND DEFINITIONS

We consider uplink in a network with n mobiles, or transmitters, and n corresponding base stations, or receivers.

Anders Möller is supported by the Center for Industrial and Applied Mathematics (CIAM) and the Royal Swedish Academy of Sciences. Ulf T. Jönsson is supported by the Swedish Research Council (VR) and the ACCESS Linnaeus Centre at KTH.

By considering the uplink as transmitter-receiver pairs, where mobile i is connected to base station i , there is no difference if, for example, there is one base station operating all users, or if every mobile is operated by different base stations. Let \bar{g}_{ij} be the channel gain between transmitter j and receiver i and define the channel gain matrix, \bar{G} , by $\bar{G} = [\bar{g}_{ij}]_{i,j=1}^n$. We assume that $\bar{g}_{ij} \geq 0, \forall (i, j)$ and $\bar{g}_{ii} > 0, \forall i$.

Let $\bar{p}_i \geq 0$ be the transmission power of user i and $\bar{p} = [\bar{p}_1, \dots, \bar{p}_n]^T$. We assume there is receiver noise, $\bar{\sigma}_i^2 > 0$, at receiver i and we let $\bar{\sigma}^2 = [\bar{\sigma}_1^2, \dots, \bar{\sigma}_n^2]^T$. The Signal to Interference Ratio (SIR) of user i in receiver i is

$$\bar{\gamma}_i = \frac{\bar{g}_{ii}\bar{p}_i}{\sum_{j \neq i} \bar{g}_{ij}\bar{p}_j + \bar{\sigma}_i^2},$$

where the numerator is the received signal power of user i and the denominator is the sum over interfering powers and receiver noise. The SIR of user i is related to its data rate by the Shannon capacity formula $W \log(1 + \bar{\gamma}_i)$, where W is the bandwidth of the channel.

The Rise Over Thermal (RoT) is a measurable quantity in the base stations that relate to congestion. To ensure cell coverage, there are constraints on the RoT-level. The *total load* at receiver i , $\bar{L}_{i,tot}$, is defined as

$$\bar{L}_{i,tot} = \frac{\sum_{j=1}^n \bar{g}_{ij}\bar{p}_j}{\sum_{j=1}^n \bar{g}_{ij}\bar{p}_j + \bar{\sigma}_i^2},$$

and is related to RoT through the relation $\bar{L}_{i,tot} = 1 - \frac{1}{RoT_i}$, see e.g. [8].

We use the notation $\text{diag}(x_i)$ or $\text{diag}(x)$ to denote the diagonal matrix with x_i in the diagonal elements, and we let M^i denote the i :th row of a matrix M . We sometimes use the matrix \bar{F} , which is defined componentwise by

$$\bar{F}_{ij} = \begin{cases} 0, & i = j, \\ \bar{g}_{ij}, & i \neq j. \end{cases} \quad (1)$$

We also use the matrix $\bar{\Delta} = \text{diag}(\bar{g}_{ii})$. Note that $\bar{F} = \bar{G} - \bar{\Delta}$.

III. INNER AND OUTER CONTROL ALGORITHMS

The parameters of a cellular system are constantly changing and subject to a high degree of disturbances and uncertainties. This motivates the use of control strategies to adapt to changing radio conditions and to ensure system performance. In this section we model the control loops that ensure that the congestion is limited and the QoS achieved. The system model can be seen as a cascade control system with an inner and outer control loop, see Figure 1.

The system model we derive includes high order dynamics. This makes it possible to model time delays, filters and high order control algorithms. Furthermore, in real applications of cellular systems there is a time scale difference between the loops. With an example in Section VII we will see that the time scale difference can be modelled by a high order outer loop controller.

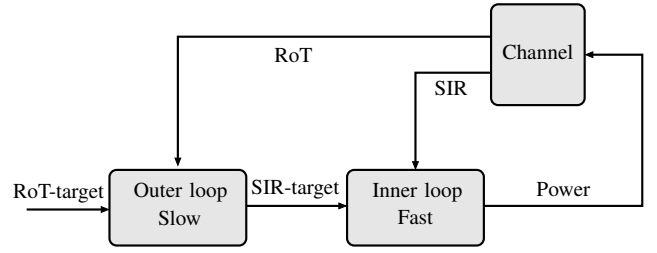


Fig. 1. Scheme over functionality of outer and inner power control loops. The outer loop controls congestion by setting the SIR target to the inner loop. The inner loop controls the SIR-level by changes in the transmission powers.

A. Inner loop

Power control algorithms for the inner power control loop has been extensively studied, see e.g. [5], [7], [6], [14], [9] or [11]. Foschini and Miljanic proposed the SIR-based Distributed Power Control (DPC) algorithm, defined by

$$\bar{p}_i[t+1] \triangleq \frac{\bar{\gamma}_i^T}{\bar{\gamma}_i[t]} \bar{p}_i[t], \quad (2)$$

where $\bar{\gamma}_i^T$ is the SIR target. Assuming that the base station knows the actual transmission power of the mobile, the DPC algorithm in (2) can be written as a linear system and easily analysed. However, in many real networks the feedback control is kept to a minimum. This means that the information exchange in the network must be distributed and the base station can typically only measure the received power, $\bar{g}_{ii}\bar{p}_i(t)$, not the individual terms.

By introducing logarithmic variables we can rewrite (2) so that the distributed nature of the information exchange is clarified. Indeed, with $p_i[t] = \ln(\bar{p}_i[t])$ and $\gamma_i^T = \ln(\bar{\gamma}_i^T)$, we can rewrite (2) as

$$p_i[t+1] = p_i[t] + (\gamma_i^T - \gamma_i[t]) \quad (3)$$

where

$$\gamma_i[t] = \ln(\bar{\gamma}_i[t]) = \ln(\bar{g}_{ii}\bar{p}_i[t]) - \ln\left(\sum_{j \neq i} \bar{g}_{ij}\bar{p}_j[t] + \bar{\sigma}_i^2\right).$$

By using the time-shift operator defined by $qp_i[t] = p_i[t+1]$, we may rewrite (3) on input output form as $p_i[t] = R(q)(\gamma_i^T - \gamma_i[t])$, where $R(q) = \frac{1}{q-1}$.

A challenge in control of cellular networks is to maintain robustness to delays. In e.g. [15] and [2] it has been shown that the DPC algorithm converges for any transmission delay of the interfering powers. However, in a cellular system there are typically no large transmission delays, but there are delays due to measuring, filtering, computations and control signalling to the mobile user. These delays can be modelled and are crucial for system stability. For example, a computational delay of size one can be modelled by $R(q) = \frac{1}{q(q-1)}$. The resulting system will then be of higher order and the convergence results in [15] are no longer applicable. An example of this can be found in e.g. [9]. We will consider

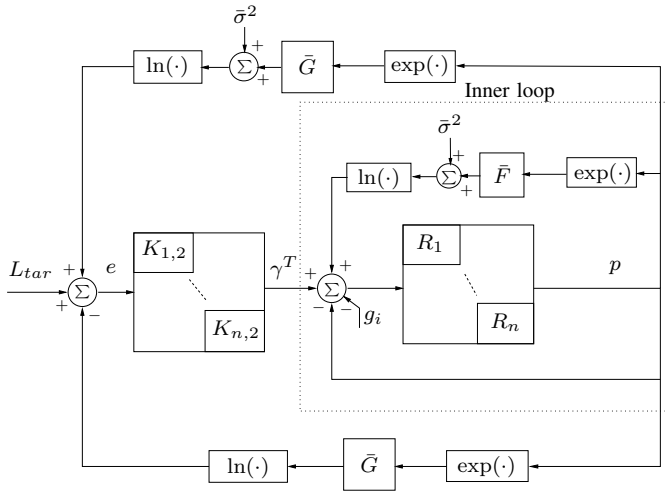


Fig. 2. Outer and inner loop in block diagram.

high order inner power control algorithms of the general form

$$p_i[t] = K_{i,1}(q) \left(\gamma_i^T - g_{ii} + \ln \left(\sum_{j \neq i} \bar{g}_{ij} \bar{p}_j[t] + \bar{\sigma}_i^2 \right) \right),$$

where $g_{ii} = \ln(\bar{g}_{ii})$, $K_{i,1}(q) = \frac{R_i(q)}{1+R_i(q)}$, which we assume to be stable, and $R_i(q) = \frac{b_{i,1}(q)}{a_{i,1}(q)}$, where $a_{i,1}(q)$ and $b_{i,1}(q)$ are polynomials in q and $a_{i,1}(q)$ is a stable polynomial. For the DPC algorithm in (3) we obtain the above form by using that $\ln(\bar{g}_{ii} \bar{p}_i[t]) = g_{ii} + p_i[t]$ and by taking $R_i(q) = \frac{1}{q-1}$. The distributed nature of the inner loop is illustrated within the dotted lines in Figure 2, where $g_i = [\ln(\bar{g}_{i1}), \dots, \ln(\bar{g}_{in})]^T$ and $\gamma^T = [\ln(\bar{\gamma}_1^T), \dots, \ln(\bar{\gamma}_n^T)]^T$.

Remark 1: Given that $R_i(q)$ has an integrator, i.e. a term $\frac{1}{q-1}$, the experienced SIR will be equal to the target SIR in the equilibrium. If there is no integrator, the equilibrium SIR will be different from the reference value given by the outer loop. The steady state properties will not be affected, since we will require an integrator in the outer loop. However, pole placement in the inner loop can be used to enhance performance.

B. Outer loop

The outer loop controls on the total load as congestion measure and dynamically sets the reference value to the inner power control loop. When the inner loop has an integrator, the reference value can be interpreted as the target SIR. Therefore we use that notation in the following derivations. We begin by defining a first order update algorithm, which we later extend to include delays and higher order control laws analogously to the inner loop model.

Define

$$\bar{L}_{i,tar} = 1 - \frac{1}{RoT_{i,tar}}$$

as the target total load. Now consider an update algorithm for $\bar{\gamma}_i^T$ in linear scale as

$$\bar{\gamma}_i^T[t+1] = \frac{\bar{L}_{i,tar}}{\bar{L}_{i,tot}[t]} \bar{\gamma}_i^T[t],$$

i.e. similar to the DPC algorithm, but with the difference that now the experienced total load is compared to the target total load.

In logarithmic scale the update algorithm can be written as

$$\gamma_i^T[t+1] = \gamma_i^T[t] + L_{i,tar} - L_{i,tot}[t],$$

where $L_{i,tar} = \ln(\bar{L}_{i,tar})$ and

$$L_{i,tot}[t] = \ln \left(\sum_{j=1}^n \bar{g}_{ij} \bar{p}_j[t] \right) - \ln \left(\sum_{j=1}^n \bar{g}_{ij} \bar{p}_j[t] + \bar{\sigma}_i^2 \right).$$

Similarly as for the inner power control loop, we consider higher order control algorithms on the following general form

$$\bar{\gamma}_i^T[t] = K_{i,2}(q) e_i[t],$$

where $K_{i,2}(q) = \frac{b_{i,2}(q)}{(q-1)a_{i,2}(q)}$, and $a_{i,2}(q)$ and $b_{i,2}(q)$ are polynomials in q , $a_{i,2}(q)$ assumed to be a stable polynomial, and where $e_i[t] = L_{i,tar} - L_{i,tot}[t]$.

The intuitive idea of controlling on total load is that if the powers increase, the total load will increase above the reference value, which will decrease the target SIR, leading to lower powers. Similarly, if the powers are low, higher powers can be allowed, raising the target SIR and eventually the powers.

The joint system model in logarithmic scale is illustrated in the block diagram in Figure 2, where $L_{tar} = [L_{1,tar}, \dots, L_{n,tar}]^T$. We note that filters for measured signals in both the inner and outer loop easily can be included in this framework, but for clarity we omit this.

IV. EQUILIBRIUM POINT

The transmission powers of the users must always be non-negative by physical constraints. Inspired by this we make the following definition.

Definition 1: The joint system is feasible if there exist finite positive powers corresponding to the target total load.

Proposition 1: Assume that $K_{i,2}(q)$ contains an integrator term for all i , $\bar{L}_{i,tar} < 1, \forall i$, and that \bar{G}^{-1} exists. Then the unique equilibrium powers, \bar{p}^* , are given by

$$\bar{p}^* = [(I - \bar{L}_{tar}) \bar{G}]^{-1} \bar{L}_{tar} \bar{\sigma}^2, \quad (4)$$

where $\bar{L}_{tar} = \text{diag}(\bar{L}_{i,tar})$. A condition for feasibility can hence be stated as

$$\bar{G}^{-1} \begin{bmatrix} \frac{\bar{L}_{1,tar}}{1-\bar{L}_{1,tar}} \bar{\sigma}_1^2 \\ \vdots \\ \frac{\bar{L}_{n,tar}}{1-\bar{L}_{n,tar}} \bar{\sigma}_n^2 \end{bmatrix} \geq 0. \quad (5)$$

Note that feasibility of the system implies that the SIRs of all users are positive in the equilibrium. This follows since the powers and all system parameters are positive. The choice of total load will determine the equilibrium point, and hence also the equilibrium SIR, $\bar{\Gamma}^* = \text{diag}(\bar{\gamma}_i^*)$. Conversely we can start with a desired equilibrium SIR and implicitly obtain a target total load assignment. The following proposition states

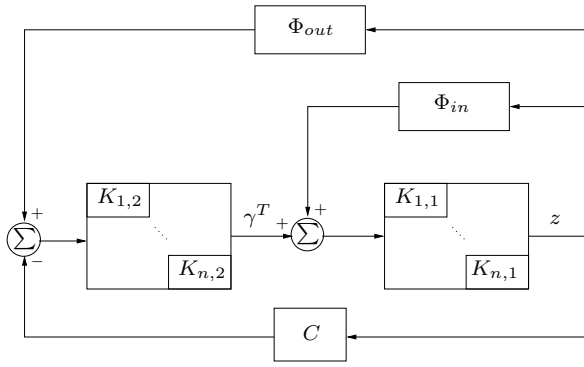


Fig. 3. Rewritten block diagram of joint outer and inner loop with an artificial lower loop with gain C .

sufficient conditions for feasibility of the joint system when starting from the SIR.

Proposition 2: Assume that $\rho(\bar{\Gamma}^* \bar{\Delta}^{-1} \bar{F}) < 1$. Then the joint system is feasible and $\bar{L}_{i,tar} < 1, \forall i$.

Note that there could be solutions to the equilibrium equation in (4) where the power vector has negative components even though $\bar{L}_{i,tar} < 1, \forall i$.

V. STABILITY ANALYSIS

The stability analysis in this section is presented in a general form, indicating that this framework is applicable for a larger problem class than the application studied. Specific problem structure will be exploited in Section VI.

We first rewrite the system to a more compact form. Then we consider the resulting blocks as operators on a Banach space. We apply input output analysis to obtain sufficient conditions for stability and convergence of the system.

The analysis is made using logarithmic scale and is based on the existence of equilibrium powers, p^* . We consider the dynamics of deviations around the equilibrium point, $z = p - p^*$, and disturbances δr .

The full system model, depicted as a block diagram in Figure 2, can equivalently be rewritten to the system in Figure 3, where an artificial lower and upper loop is added with gain C , where $C = \text{diag}(C_i)$. This results in Φ_{out} being dependent of C . Note that this way of rewriting the system is only for analysis purpose. We have used the following notation.

$$\begin{aligned} \Phi_{out}(z) &= [\Phi_{1,out}(z), \dots, \Phi_{n,out}(z)]^T \\ \Phi_{in}(z) &= [\Phi_{1,in}(z), \dots, \Phi_{n,in}(z)]^T \\ \Phi_{i,out}(z) &= \ln \left(\frac{\sum_{j=1}^n \bar{g}_{ij} e^{p_j^*} e^{z_j} + \bar{\sigma}_i^2}{\sum_{j=1}^n \bar{g}_{ij} e^{p_j^*} e^{z_j}} \right) + C_i z_i + L_{i,tar} \\ \Phi_{i,in}(z) &= \ln \left(\sum_{j \neq i} \bar{g}_{ij} e^{p_j^*} e^{z_j} + \bar{\sigma}_i^2 \right) - \gamma_i^T(p^*) + g_{ii} + p_i^* \\ K_1(q) &= \text{diag}(R_i(q)/(1 + R_i(q))), \quad K_2(q) = \text{diag}(K_{i,2}). \end{aligned}$$

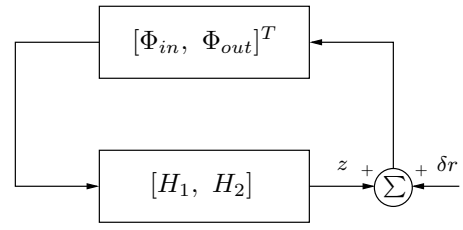


Fig. 4. Input output form of the joint system.

We now further rewrite the system to input output form, see Figure 4, where

$$\begin{aligned} H_1(q) &= [I + K_1(q)K_2(q)C]^{-1} K_1(q) \\ H_2(q) &= [I + K_1(q)K_2(q)C]^{-1} K_1(q)K_2(q). \end{aligned}$$

The analysis will be performed in the following signal spaces

- (i) $l_\infty^n = \{z : N \rightarrow R_\infty^n : \|z\|_\infty < \infty\}$
- (ii) $l_{2,\infty}^n = \{z : N \rightarrow R_\infty^n : \|z\|_{2,\infty} < \infty\}$

where the norms are defined as $\|z\|_\infty = \sup_k |z[k]|_\infty$ and $\|z\|_{2,\infty} = (\sum_{k=0}^\infty |z[k]|_\infty^2)^{1/2}$. The spatial dimension will often be suppressed. It has previously been established that use of the l_2 -space is not appropriate for this kind of analysis, see e.g. [10] or [11] for a further discussion on choice of signal spaces.

Let F be a nonlinear operator $F : X \rightarrow X$ such that $F(0) = 0$ and X is a normed vector space. Then the global Lipschitz constant is defined as

$$L[F; X] \triangleq \sup_{z_1, z_2 \in X, z_1 \neq z_2} \frac{\|F(z_1) - F(z_2)\|_X}{\|z_1 - z_2\|_X},$$

where $\|\cdot\|_X$ denotes the norm on X . For us it will be interesting to consider the Lipschitz constant on a subset B_X of X defined by how large deviations around the equilibrium we consider. Define

$$L[F; B_X] \triangleq \sup_{z_1, z_2 \in B_X, z_1 \neq z_2} \frac{\|F(z_1) - F(z_2)\|_X}{\|z_1 - z_2\|_X}.$$

For linear operators the gain and Lipschitz constants coincide. The l_1 -norm of a linear system H_i is defined as

$$\|H_i\|_1 \triangleq \sum_{k=0}^{\infty} |h_i[k]|,$$

where $h_i[k]$ is the impulse response at time k . For a diagonal matrix H , $H(q) = \text{diag}(H_i)$, the induced norms from l_∞ and $l_{2,\infty}$ become (see e.g. [4])

$$\|H\|_{l_\infty \rightarrow l_\infty} = \|H\|_1 \triangleq \max(\|H_1\|_1, \dots, \|H_n\|_1)$$

$$\|H\|_{l_{2,\infty} \rightarrow l_{2,\infty}} \leq \|H\|_{1,1} \triangleq \sum_{k=0}^{\infty} |h[k]|_1,$$

where we used the matrix norm $\|M\|_1 = |M|_{R_\infty^n \rightarrow R_\infty^n} = \max_{1 \leq i \leq n} \sum_{j=1}^n |M_{ij}|$. Clearly $\|H\|_1 \leq \|H\|_{1,1}$, and equality holds if $H_i = H_j, \forall (i, j)$.

Let X be either of the spaces l_∞^n or $l_{2,\infty}^n$. Consider the set B , defined componentwise by $p_{\min,i} \leq p_i \leq p_{\max,i}, \forall i$,

where $p_{\min,i}, p_{\max,i}$ are lower and upper bounds on the transmission powers of the users. The induced sets for the deviations around the equilibrium point, z , is then given by

$$B^* = \{z \in \mathbf{R}_\infty^n : p_{\min,i} - p_i^* \leq z_i \leq p_{\max,i} - p_i^*, \forall i\} \quad (6)$$

$$B_X^* = \{z \in X : z[k] \in B^*, \forall k\}. \quad (7)$$

For our analysis we need to consider the maximum interior balls in B^* and B_X^* , which are defined as

$$B^*(\gamma) = \{z \in \mathbf{R}_\infty^n : |z|_\infty \leq \gamma\},$$

$$B_X^*(\gamma) = \{z \in X : z[k] \in B^*(\gamma), \forall k\},$$

where $\gamma = \min_i \{\min\{p_i^* - p_{\min,i}, p_{\max,i} - p_i^*\}\}$.

Proposition 3:

$$\begin{aligned} L[\Phi_{in}; B_{l_\infty}^*(\gamma)] &= L[\Phi_{in}; B_{l_{2,\infty}}^*(\gamma)] = L[\Phi_{in}; B^*(\gamma)] \\ &= \max_{z \in B^*(\gamma)} |\nabla \Phi_{in}(z)|_1 \\ &= \max_i \frac{\bar{F}^i e^{p^* + z_{\max}}}{\bar{\sigma}_i^2 + \bar{F}^i e^{p^* + z_{\max}}} < 1, \end{aligned}$$

where $e^{p^* + z_{\max}} = [e^{p_1^* + z_{\max,1}}, \dots, e^{p_n^* + z_{\max,n}}]$ and $z_{\max,i} = p_{\max,i} - p_i^*, \forall i$.

Proof: See [10] or [11]. ■

Proposition 4:

$$\begin{aligned} L[\Phi_{out}; B_{l_\infty}^*(\gamma)] &= L[\Phi_{out}; B_{l_{2,\infty}}^*(\gamma)] = L[\Phi_{out}; B^*(\gamma)] \\ &= \max_{z \in B^*(\gamma)} |\nabla \Phi_{out}(z)|_1 \\ &= \max_i \max_{z \in B^*(\gamma)} \left(\frac{\bar{\sigma}_i^2 \bar{F}^i e^{p^* + z}}{(\bar{G}^i e^{p^* + z} + \bar{\sigma}_i^2)(\bar{G}^i e^{p^* + z})} \right. \\ &\quad \left. + \left| C_i - \frac{\bar{\sigma}_i^2 \bar{g}_{ii} e^{p_i^*}}{(\bar{G}^i e^{p^* + z} + \bar{\sigma}_i^2)(\bar{G}^i e^{p^* + z})} \right| \right) \end{aligned}$$

Proof: The proof follows the lines of Proposition 3. ■

Note that the Lipschitz constant depends on the value of the parameter C .

We are now ready for our main theorem on stability.

Theorem 1: Assume that

$$\|H_1\|_1 L[\Phi_{in}; B^*(\gamma)] + \|H_2\|_1 L[\Phi_{out}; B^*(\gamma)] < 1,$$

then there exists a unique power trajectory $z \in B_{l_\infty}^*(\gamma)$ for all

$$\begin{aligned} \|\delta r\|_\infty &\leq \gamma \left(1 - \|H_1\|_1 L[\Phi_{in}; B^*(\gamma)] \right. \\ &\quad \left. - \|H_2\|_1 L[\Phi_{out}; B^*(\gamma)] \right). \end{aligned} \quad (8)$$

If it in addition holds that $\|\delta r\|_{l_{2,\infty}} < \infty$ and that

$$\begin{aligned} \|H_1\|_{l_{2,\infty} \rightarrow l_{2,\infty}} L[\Phi_{in}; B^*(\gamma)] \\ + \|H_2\|_{l_{2,\infty} \rightarrow l_{2,\infty}} L[\Phi_{out}; B^*(\gamma)] < 1, \end{aligned}$$

then $p[k] \rightarrow p^*$ as $k \rightarrow \infty$.

Proof: The proof follows the lines of Theorem 1 in [11]. ■

Remark 2: In the analysis we rewrite the system by introducing the direct feedback with gain C to the dynamics part of the block diagram, see Figure 3. This loop transformation is needed, since the l_1 -norm of the integrator in K_2 is infinite.

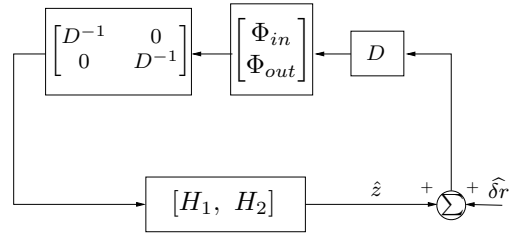


Fig. 5. Input output form of the joint scaled system.

VI. SCALING MULTIPLIERS AND LOCAL ANALYSIS

Structure of the problem can be exploited by introducing scaling multipliers, see Figure 5. This gives the transformed but equivalent system where

$$\hat{H}_1(q) \triangleq D^{-1} H_1(q) D = H_1(q)$$

$$\hat{H}_2(q) \triangleq D^{-1} H_2(q) D = H_2(q)$$

$$\hat{\Phi}_{in}(\hat{z}) \triangleq D^{-1} \Phi_{in}(D\hat{z}), \quad \hat{\Phi}_{out}(\hat{z}) \triangleq D^{-1} \Phi_{out}(D\hat{z})$$

$$\hat{\delta r} \triangleq D^{-1} \delta r, \quad \hat{z} \triangleq D^{-1} z$$

for any $D \in \mathcal{D} = \{D = \text{diag}(d_1, \dots, d_n) : d_k > 0\}$.

Proposition 5: The scaled nonlinearities $\hat{\Phi}_{in} : \mathbf{R}_\infty^n \rightarrow \mathbf{R}_\infty^n$ and $\hat{\Phi}_{out} : \mathbf{R}_\infty^n \rightarrow \mathbf{R}_\infty^n$ are Lipschitz on $D^{-1} B^* \subset \mathbf{R}_\infty^n$ with

$$L[\hat{\Phi}_{in}; D^{-1} B^*] = \max_{z \in B^*} |D^{-1} \nabla \Phi_{in}(z) D|_1 \triangleq L_D^{in}$$

$$L[\hat{\Phi}_{out}; D^{-1} B^*] = \max_{z \in B^*} |D^{-1} \nabla \Phi_{out}(z) D|_1 \triangleq L_D^{out}$$

Proof: The proof follows the lines of Proposition 4 and Proposition 5 in [11]. ■

To get to our stability result in the scaled signal space we need to consider the Lipschitz constants for the signal spaces previously defined. Define

$$\hat{\gamma} = \min_i \left\{ \min \left\{ \frac{1}{d_i} (p_i^* - p_{\min,i}), \frac{1}{d_i} (p_{\max,i} - p_i^*) \right\} \right\},$$

and the sets

$$C(\hat{\gamma}) = \{z \in \mathbf{R}_\infty^n : -d_i \hat{\gamma} \leq z_i \leq d_i \hat{\gamma}, \forall i\}$$

$$C_X(\hat{\gamma}) = \{z \in X : z[k] \in C(\hat{\gamma}), \forall k\}$$

$$\begin{aligned} C_{\delta,X}(\hat{\gamma}) &= \left\{ \delta r \in X : |\delta r_i[k]| \leq \hat{\gamma} d_i \left(1 - \|H_1\|_1 L_D^{in} \right. \right. \\ &\quad \left. \left. - \|H_2\|_1 L_D^{out} \right), \forall (i, k) \right\} \end{aligned}$$

Proposition 6: The scaled nonlinearities $\hat{\Phi}_{in} : X \rightarrow X$ and $\hat{\Phi}_{out} : X \rightarrow X$ are Lipschitz on $C_X(\hat{\gamma})$ with

$$\begin{aligned} L[\hat{\Phi}_{in}; C_{l_\infty}(\hat{\gamma})] &= L[\hat{\Phi}_{in}; C_{l_{2,\infty}}(\hat{\gamma})] = L[\hat{\Phi}_{in}; C(\hat{\gamma})] \\ &\leq \max_{z \in B^*} |D^{-1} \nabla \Phi_{in}(z) D|_1 = L_D^{in} \end{aligned}$$

$$\begin{aligned} L[\hat{\Phi}_{out}; C_{l_\infty}(\hat{\gamma})] &= L[\hat{\Phi}_{out}; C_{l_{2,\infty}}(\hat{\gamma})] = L[\hat{\Phi}_{out}; C(\hat{\gamma})] \\ &\leq \max_{z \in B^*} |D^{-1} \nabla \Phi_{out}(z) D|_1 = L_D^{out} \end{aligned}$$

Proof: A proof can be found in [11]. ■

We can now give conditions for stability.

Corollary 1: If

$$\|H_1\|_1 L_D^{in} + \|H_2\|_1 L_D^{out} < 1,$$

then there exists a unique power distribution $z \in C_{l_\infty}(\hat{\gamma})$ for all $\delta r \in C_{\delta, l_\infty}(\hat{\gamma})$.

If it in addition holds that $\|\delta r\|_{2, \infty} < \infty$ and

$$\|H_1\|_{l_{2, \infty} \rightarrow l_{2, \infty}} L_D^{in} + \|H_2\|_{l_{2, \infty} \rightarrow l_{2, \infty}} L_D^{out} < 1,$$

then $z[k] \rightarrow 0$ as $k \rightarrow \infty$.

Proof: We study stability in the scaled signal space, where $\hat{z} = D^{-1}z$, $z \in C_{l_\infty}(\hat{\gamma})$ implies that $\hat{z} \in B_{l_\infty}^*(\hat{\gamma})$ and $\delta r \in C_{\delta, l_\infty}(\hat{\gamma})$ implies that

$$\|\hat{\delta r}\|_\infty \leq \hat{\gamma} \left(1 - \|H_1\|_1 L_D^{in} - \|H_2\|_1 L_D^{out}\right).$$

Theorem 1 then proves the statement. \blacksquare

We will now use more structure of the specific problem by an analysis of the nonlinearities around the equilibrium point. Note that

$$\bar{\gamma}_i(z) = \frac{\bar{g}_{ii} e^{p_i^* + z_i}}{\bar{\sigma}_i^2 + \bar{F}^i e^{p_i^* + z_i}}.$$

Proposition 7:

$$\sigma(\nabla \Phi_{in}(z)) = \sigma(\bar{\Gamma}(z) \bar{\Delta}^{-1} \bar{F}),$$

where $\sigma(\cdot)$ denotes the spectrum of a matrix.

Remark 3: The result implies that in the equilibrium point, the Jacobian of the inner power control loop has the same eigenvalues as the matrix determining feasibility of the inner loop.

Now consider $\nabla \Phi_{out}$ in the equilibrium point, where $z = 0$, with the choice

$$C_i = \frac{\bar{\sigma}_i^2 \bar{g}_{ii} e^{p_i^*}}{(\bar{G}^i e^{p_i^*} + \bar{\sigma}_i^2)(\bar{G}^i e^{p_i^*})}, \quad \forall i, \quad (9)$$

which implies that the diagonal elements are cancelled.

Proposition 8:

$$\sigma(\nabla \Phi_{out}(0)) = \sigma\left(\text{diag}\left(\frac{\bar{L}_{i,tar} - 1}{\bar{L}_{i,tar}}\right) \text{diag}\left(\frac{\bar{\gamma}_i^*}{\bar{\gamma}_i^* + 1}\right) \bar{\Delta}^{-1} \bar{F}\right)$$

For clarity of notation, denote the scaled Lipschitz constants around the equilibrium point, $z = 0$,

$$\begin{aligned} L_D^{in}(0) &\triangleq L[\hat{\Phi}_{in}; D^{-1}B^*(0)] \\ L_D^{out}(0) &\triangleq L[\hat{\Phi}_{out}; D^{-1}B^*(0)]. \end{aligned}$$

We have

$$L_D^{in}(0) = \inf_{D \in \mathcal{D}} |D^{-1} \nabla \Phi_{in}(0) D|_1 = \rho(\nabla \Phi_{in}(0))$$

$$L_D^{out}(0) = \inf_{D \in \mathcal{D}} |D^{-1} \nabla \Phi_{out}(0) D|_1 = \rho(|\nabla \Phi_{out}(0)|)$$

where $\rho(\cdot)$ is the spectral radius and $|\cdot|$ means component-wise absolute value.

Theorem 2: Let the scalings, D , be given by the eigenvector corresponding to $\rho(\nabla \Phi_{in}(0))$, taken positive. Then a sufficient condition for local stability is given by

$$\left(\|H_1\|_1 + \|H_2\|_1 \max_i \left| \frac{\bar{L}_{i,tar} - 1}{\bar{L}_{i,tar}(\bar{\gamma}_i^* + 1)} \right| \right) \rho(\bar{\Gamma}^* \bar{\Delta}^{-1} \bar{F}) < 1. \quad (10)$$

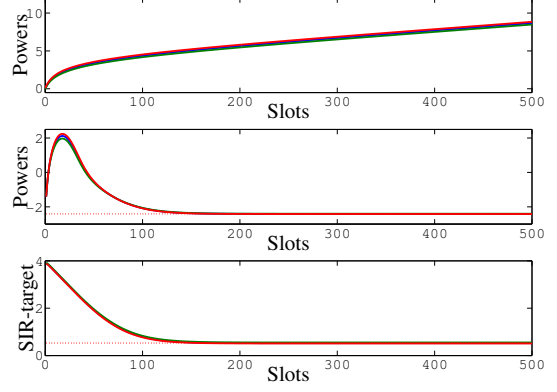


Fig. 6. The simulation illustrates that a power rush due to infeasibility of the inner loop is stopped. In the upper plot we see a power rush of the inner loop, where no outer loop is applied. In the middle and lower plot the outer loop is applied. We can see that the transmission powers initially increase, but, as the SIR-target is decreased, the powers also decrease and the system is stabilized. The system converges to the equilibrium point determined by the target total load.

Proof: The proof is based on Corollary 1, Proposition 7 and the fact that $\nabla \Phi_{out}(0)$ can be written as a function of $\nabla \Phi_{in}(0)$. \blacksquare

Remark 4: The choice of scalings in the theorem above corresponds to the optimal scalings with respect to minimization of $L_D^{in}(0)$. A similar criterion can be made by optimizing the scalings with respect to the outer loop. However, for systems operating with high throughput, the nonlinear feedback corresponding to the inner loop is high and seems to be more critical for stability.

VII. PREVENTION OF POWER RUSHES

A cause of power rushes is when the SIR-target is set too high and the users start competing with increasing transmission powers. This problem is often avoided in the literature by only considering feasible networks. Consider the following example where

$$\bar{G} = \begin{bmatrix} 1 & 0.025 & 0.01 \\ 0.015 & 1 & 0.01 \\ 0.03 & 0.01 & 1 \end{bmatrix}, \quad \bar{\sigma}^2 = \begin{bmatrix} 0.05 \\ 0.05 \\ 0.05 \end{bmatrix},$$

and let the controllers be given by

$$R(q) = \frac{\beta}{q-1}, \quad K_2(q) = \frac{K_I}{q-1},$$

where $\beta = 0.3$ and $K_I = 0.07$ for all users. The maximal common feasible SIR target is given by the limit $\frac{1}{\rho(\bar{\Delta}^{-1} \bar{F})} \approx 30.8$, i.e. $\gamma_i^T \approx 3.4$ in logarithmic scale. In the upper plot of Figure 6 we see that the inner loop, with unchanged SIR-target, leads to a power rush. When applying the outer loop control to the system, initialized with the same SIR-target and $\bar{L}_{i,tar} = 0.65$, $\forall i$, the system is stabilized, see the middle and lower plot of Figure 6.

Using the stability condition in Theorem 2, the joint system gain can be computed to $0.13 < 1$, and local stability

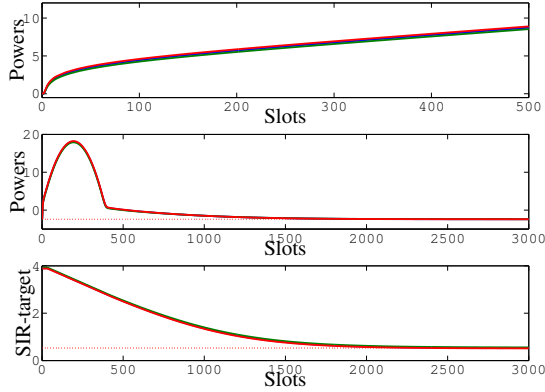


Fig. 7. Simulation of a WCDMA model with time delays and time scale modelling. The same parameters as in Figure 6 were used. We can see that the behaviour is similar, but on a much slower and larger scale.

can be verified. In this case local stability can be guaranteed for $\bar{L}_{i,tar}$ up to about 0.97.

Now consider the same example for a WCDMA network. There are typically two time delays in the inner control loop and 15 in the outer control loop. Furthermore there is a timescale difference of about 15. We model this by a chain of operations. First a low pass filter is applied to the error, $e[t] = L_{tar} - L_{tot}[t]$, to avoid aliasing. Then downsampling is made by taking every 15:th sample. On this slower time scale the outer loop controller is applied. The output of the controller is then upsampled by keeping the output constant for 15 time slots. The time domain operations correspond to the following transfer function of the outer loop

$$K_2(z) = \hat{K}_0(z^{15})\hat{L}(z)\left(\frac{1 - z^{-15}}{1 - z^{-1}}\right),$$

where $\hat{K}_0(z)$ and $\hat{L}(z)$ are the z-transforms of the outer loop controller and the low pass filter respectively. Replacing z with q , applying $\hat{K}_0(q) = \frac{K_I}{q-1}$ and the inner and outer loop delays gives

$$K_2(q) = \frac{K_I}{q^{29}(q-1)}\hat{L}(q), \quad \text{and} \quad R(q) = \frac{\beta}{q^2(q-1)}.$$

The simulations in Figure 7 shows a similar behaviour to the previous example. Now, however, the system reacts slower, which implies that the power rush is stopped later and the powers reach higher values. As before we can use Theorem 2 to study local stability. For $\bar{L}_{i,tar} = 0.65$, $\forall i$, we have the joint system gain $0.46 < 1$, and hence the system is stable around the equilibrium point. Now, however, the maximum value of $\bar{L}_{i,tar}$ for which local stability can be verified by Theorem 2 is 0.88.

As illustrated by the examples above, infeasibility of the inner loop leads to power rushes. This raises the question what happens when the joint system is infeasible. Infeasibility implies that the total load targets cannot be fulfilled for all users. This means that for at least one user, the experienced total load is higher than the target total load. In the ideal

case, the outer loop controller will then continuously lower the SIR, which will lead to decreasing transmission powers of the user. This will eventually lead to that the user leaves the system, making it in a sense self-regulating. This is an interesting and desirable property.

VIII. CONCLUSIONS

In this paper we introduce a framework that can be used to model control in a wireless cellular network. It is based on distributed high order algorithms that use measurable data for feedback. Modelling of filters, delays and time-scale differences is straightforward to include. We perform stability analysis of the nonlinear system and give sufficient conditions for stability. The results are sharpened and structure of the problem revealed. Simulations indicate that the model has advantageous properties.

REFERENCES

- [1] M. Abbas-Turki, F. de S. Chaves, H. Abou-Kandil, and J. M. T. Romano. Mixed h2/h power control with adaptive qos for wireless communication networks. In *Proc. of the 10th European Control Conference (ECC'09)*, Budapest, Hungary, 2009.
- [2] T. Charalambous, I. Lestas, and G. Vinnicombe. On the stability of the Foschini-Miljanic algorithm with time-delays. In *Proceedings of the 47th IEEE Conference on Decision and Control*, Cancun, Mexico, 2008.
- [3] M. Chiang, P. Hande, T. Lan, and C.W. Tan. Power control in wireless cellular networks. *Foundations and Trends in Communications and Information Theory*, 2(4):1–156, 2008.
- [4] M.A. Dahleh and I. Diaz-Bobillo. *Control of Uncertain Systems: A Linear Programming Approach*. Prentice-Hall, 1995.
- [5] G. J. Foschini and Z. Miljanic. Distributed autonomous wireless channel assignment algorithm with power control. *IEEE Transactions on Vehicular Technology*, 44(3):420–429, 1995.
- [6] F. Gunnarsson. *Power Control in Cellular Radio Systems: Analysis, Design and Estimation*. PhD thesis, Linköping University, Linköping, Sweden, 2000.
- [7] F. Gunnarsson and F. Gustafsson. Control theory aspects of power control in UMTS. *Control Engineering Practice*, 11(10):1113–1125, 2003.
- [8] E. Gejjer Lundin and F. Gunnarsson. Uplink load in cdma cellular radio systems. *IEEE Transactions on Vehicular Technology*, 55(4):1331 – 1346, 2006.
- [9] A. Möller and U. T. Jönsson. Stability of high order distributed power control. In *Proceedings of the 48th IEEE Conference on Decision and Control*, Shanghai, China, 2009.
- [10] A. Möller and U. T. Jönsson. Stability of systems under interference feedback. In *Proceedings of the European Control Conference*, Budapest, Hungary, 2009.
- [11] A. Möller and U. T. Jönsson. Input output analysis of power control in wireless networks. Technical Report TRITA-MAT-10-OS03, Dept. of Mathematics, Royal Inst. of Technology, September 2010. A short version appeared in Proceedings of the 49th IEEE Conference on Decision and Control.
- [12] A. Möller, U. T. Jönsson, Mats Blomgren, and Fredrik Gunnarsson. Stability of rate and power control algorithms in wireless cellular networks. Technical Report TRITA-MAT-11-OS07, Dept. of Mathematics, Royal Inst. of Technology, August 2011.
- [13] Subramanian and A.H. A.; Sayed. Joint rate and power control algorithms for wireless networks. *IEEE Transactions on Signal Processing*, 53(11):4204–4214, 2005.
- [14] C. W. Sung and K.-K. Leung. A generalized framework for distributed power control in wireless networks. *IEEE Transactions on Information Theory*, 51(7):2625–2635, 2005.
- [15] R.D. Yates. A framework for uplink power control in cellular radio systems. *IEEE Journal on selected areas in communications*, 13(7):1341–1347, 1995.